iScience

CellPress
OPEN ACCESS

Article

Discovery of a microbial rhodopsin that is the most stable in extreme environments

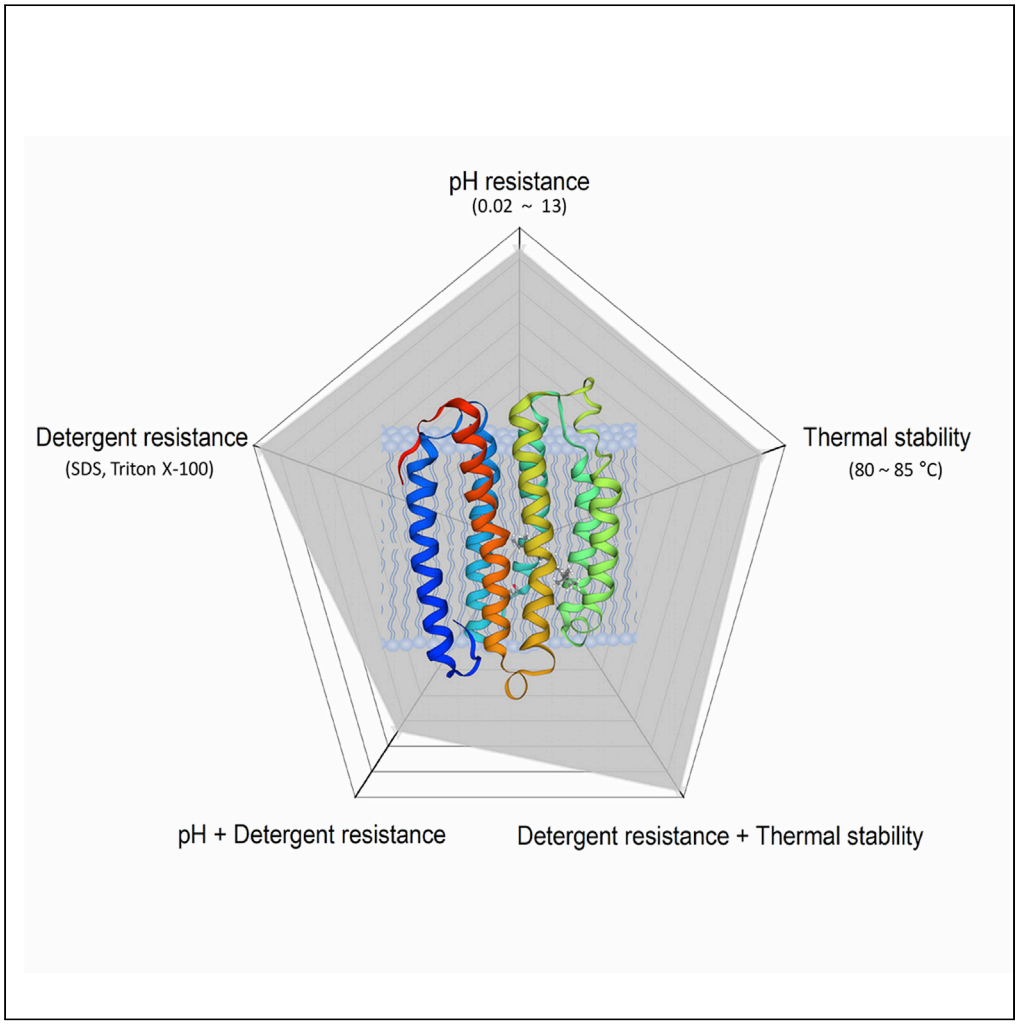

Jin-gon Shim, Veasna Soum, Kun-Wook Kang, ..., Alina Pushkarev, Kwanwoo Shin, Kwang-Hwan Jung

kjung@sogang.ac.kr

Highlights

Tara76 rhodopsin showed strong stability against pH, temperature, detergents, dried, and salt

Tara76 rhodopsin is stable under dual and triple stress conditions

Electrical properties were measured at high temperature using the membrane protein

The hydrophobicity of helix E and the Schiff base influence the stability of rhodopsin

Shim et al., iScience 24, 102620
June 25, 2021
https://doi.org/10.1016/j.isci.2021.102620

iScience

CellPress
OPEN ACCESS

Article

Discovery of a microbial rhodopsin that is the most stable in extreme environments

Jin-gon Shim,[1] Veasna Soum,[2] Kun-Wook Kang,[1] Kimleng Chuon,[1] Shin-Gyu Cho,[1] Ji-Hyun Kim,[1] Seanghun Meas,[1] Alina Pushkarev,[3] Kwanwoo Shin,[2] and Kwang-Hwan Jung[1,4,*]

SUMMARY

Microbial rhodopsin is a retinal protein that functions as an ion pump, channel, and sensory transducer, as well as a light sensor, as in biosensors and biochips. Tara76 rhodopsin is a typical proton-pumping rhodopsin that exhibits strong stability against extreme pH, detergent, temperature, salt stress, and dehydration stress and even under dual and triple conditions. Tara76 rhodopsin has a thermal stability approximately 20 times higher than that of thermal rhodopsin at 80°C and is even stable at 85°C. Tara76 rhodopsin is also stable at pH 0.02 to 13 and exhibits strong resistance in detergent, including Triton X-100 and SDS. We tested the current flow that electrical current flow across dried proteins on the paper at high temperatures using an electrode device, which was measured stably from 25°C up to 120°C. These properties suggest that this Tara76 rhodopsin is suitable for many applications in the fields of bioengineering and biotechnology.

INTRODUCTION

Microbial rhodopsin is a membrane protein with retinal as a chromophore and plays various roles through light stimulation (Ernst et al., 2014). Metagenomic studies of microbial rhodopsin have shown that up to 50% of microbial rhodopsins are found on land and in coastal organisms (Finkel et al., 2013). Thus, the abundance of microbial rhodopsin distribution is an important evolutionary product in living organisms for adapting to the environment. As seven-alpha helix transmembrane proteins, microbial rhodopsins induce retinal isomerization by light and function in ion transport and as channels and light sensors (Béjà et al., 2000; Spudich and Luecke, 2002; Yoshida et al., 2017). Various types of rhodopsins such as bacteriorhodopsin (BR), halorhodopsin (HR), proteorhodopsin (PR), and channel rhodopsin (ChR) have been reported and studied (Friedrich et al., 2002; Schobert and Lanyi, 1982).

Proton-transporting rhodopsins have been studied for various functions, including the existing outward proton pump function and new functions, such as inward proton pump and cation channel (Govorunova et al., 2015; Inoue et al., 2016a). Other studies have reported conversion from protons to other ions and a transition from pumping to ChR. This function is not a natural function but occurs through the mutation of specific residues (Govorunova et al., 2015; Hasemi et al., 2016; Inoue et al., 2016a, 2016b; Vogt et al., 2015). In addition, a new type of heliorhodopsin with unknown function has been reported (Pushkarev et al., 2018b). Since microbial rhodopsins can be controlled functionally by light, they are applied as an optogenetic tool. Several *in vivo* experiments have been reported with microbial rhodopsin to control the target neurotransmitter ion and serve as an effective optogenetic silencer and activator (Glock et al., 2015; Govorunova et al., 2015; Govorunova and Koppel, 2016; Hoque et al., 2016; McIsaac et al., 2015). In addition to optogenetic studies, the use of enzyme rhodopsin rather than pump or ChR has been reported to increase the diversity of microbial rhodopsin. Furthermore, application research is being conducted into biosensors since bioelectronic devices based on BR from *Halobacterium salinarum* have been reported (Li et al., 2018; McIsaac et al., 2015; Tsunoda et al., 2021; Yoshida et al., 2017). BR has also been studied for photochemical and photoelectric applications such as immune sensors, photovoltaic cells, and artificial retinal prostheses (Li et al., 2018).

Research on microbial rhodopsin is increasing not only regarding functional research on photochemical reaction centers but also pertaining to proteomics research. Thermophilic rhodopsin (TR) is derived from an extreme thermophilic bacterium, *Thermus thermophilus* JL-18 (Tsukamoto et al., 2013). TR has been found in hot springs at approximately 75°C, suggesting that it is functional as a stable protein at a high

[1]Department of Life Science and Institute of Biological Interfaces, Sogang University, Seoul 04107, Korea

[2]Department of Chemistry, Sogang University, Seoul 04107, Korea

[3]Faculty of Biology, Technion – Israel Institute of Technology, Haifa 32000, Israel

[4]Lead contact

*Correspondence: kjung@sogang.ac.kr

https://doi.org/10.1016/j.isci.2021.102620

temperature, which is important for essential stability on proteins. These TRs have been reported to be stable and functional at high temperatures, and they may be valuable optogenetic tools as light sensors. Recently, an oligomeric state was reported for the lipid state of TR, which is monomeric at high temperatures and has strong stability (Shionoya et al., 2018; Tsukamoto et al, 2013, 2016). In addition, RxR found in *Rubrobacter xylanophilus* DSM 9941^T exhibits high thermal stability (85°C for 10 h) (Kanehara et al., 2017). Other physical properties have been studied. *Leptosphaeria* rhodopsin exists in an oligomeric state and exhibits resistance to detergents (Ji et al., 2017).

Microbial rhodopsin found in *Coccomyxa subellipsoidea* of eukaryotic origin exhibits both temperature and detergent stability (Ranjan and Kateriya, 2018). In the case of *Np*SRII, it was stable in a relatively wide pH and temperature range. Studies of these various physical factors can be expanded to many possible applications (Grote et al., 2014; Hirayama et al., 1992; Ranjan and Kateriya, 2018). The physical resistance of proteins has been studied for numerous factors, including the effect of micelle structure, ionic strength, pH, temperature, and oxidation. However, the proteins reported to be stable for several factors are generally not stable under all stressful conditions. Therefore, the stability of complex and specific factors must be improved for industrial and academic applications (Ece et al., 2015; Foit et al., 2009; Magliery, 2015; Otzen, 2002). Mutagenesis may also be used to improve stability (Foit et al., 2009).

In this study, we tested the biochemical and biophysical resistance of a new rhodopsin originally found as a partial sequence in a chimeric construct where the partial rhodopsin was obtained from a depth of 100 m (Pushkarev et al., 2018a). The full protein sequence was obtained by screening the Tara project with the partial sequence as bait. The full sequence belonged to an uncultured bacterium. Tara76 rhodopsin was isolated from 76 stations of the Tara ocean expedition in which the oceanomics project collected tens of thousands of biological samples. We compared the stability of Tara76 rhodopsin to other representative rhodopsins, including PR, *Gloeobacter violaceus* rhodopsin (GR), and TR.

RESULTS

Expression and characterization of Tara76 rhodopsin

Tara76 rhodopsin found in uncultured bacteria has a DTE (Asp97, Thr101, Glu108) motif similar to PR. In addition, L105 in GPR (green light-absorbing PR), which is reported as a color tuning residue, has glutamine in BPR (blue light-absorbing PR) (Figure S1). The protein size is 232 amino acids, which is smaller than that of BR, GPR, and BPR. When various microbial rhodopsins and Tara76 rhodopsin were subjected to phylogenetic analysis, Tara76 rhodopsin closely aligned with TR near the upper group of PR (Figure 1A). Tara76 rhodopsin had a maximum absorption of 489 nm, similar to BPR, at neutral pH 7, and the color was orange. At pH 0.02, it red shifted to 517 nm, then to 527 nm at pH 4, to 489 nm at pH 10 (same with wild-type [WT]), and again to 526 nm at pH 13 (Figure 1B). This shows that Tara76 rhodopsin is very stable at various pH values, which was confirmed by the absorption spectra at various pH values; when the acidic condition changed from pH 7 to pH 4, it blue shifted according to the pH condition up to 527 nm. This tendency was reversed when the pH decreased; when the pH was lowered to 0.02 from pH 4 (527 nm), a blue shift to 517 nm was observed.

Just like the pumping rhodopsin, this characteristic shift of Tara76 rhodopsin in each pH range will have pKa values according to the interval trend of the spectral shift. This was confirmed by obtaining pKa values: from pH 0.02 to 4, pKa = 1.77 (Figure 1G); from pH 4 to 9.5, pKa = 5.26 (Figure 1H); and from pH 10 to 13, pKa = 10.95 (Figure 1I). The protein is expected to be stable and have pumping activity under extreme pH conditions. Tara76 rhodopsin exhibited proton-pumping activity at pH 2 (Figure S2A). The y axis represents the amount of change in pH, and it showed a high amount of proton movement because of low pH condition even though a low scale of the proton. When the amount of transported proton was calculated, a large amount of proton was transported at low pH. It showed fast transportability for cells to respond to low external pH (Figure S2B).

The pumping activity of Tara76 rhodopsin was compared to that of GR and PR (Figure S3), showing that Tara76 rhodopsin moved fewer protons than GR but more protons than PR. To compare the same amount of rhodopsin, we obtained the bar values by dividing the amount of moved protons with the amount of purified protein after the measurement (Figure S3B). This pumping efficiency indicates that Tara76 rhodopsin can function as a proton-pumping rhodopsin in general.

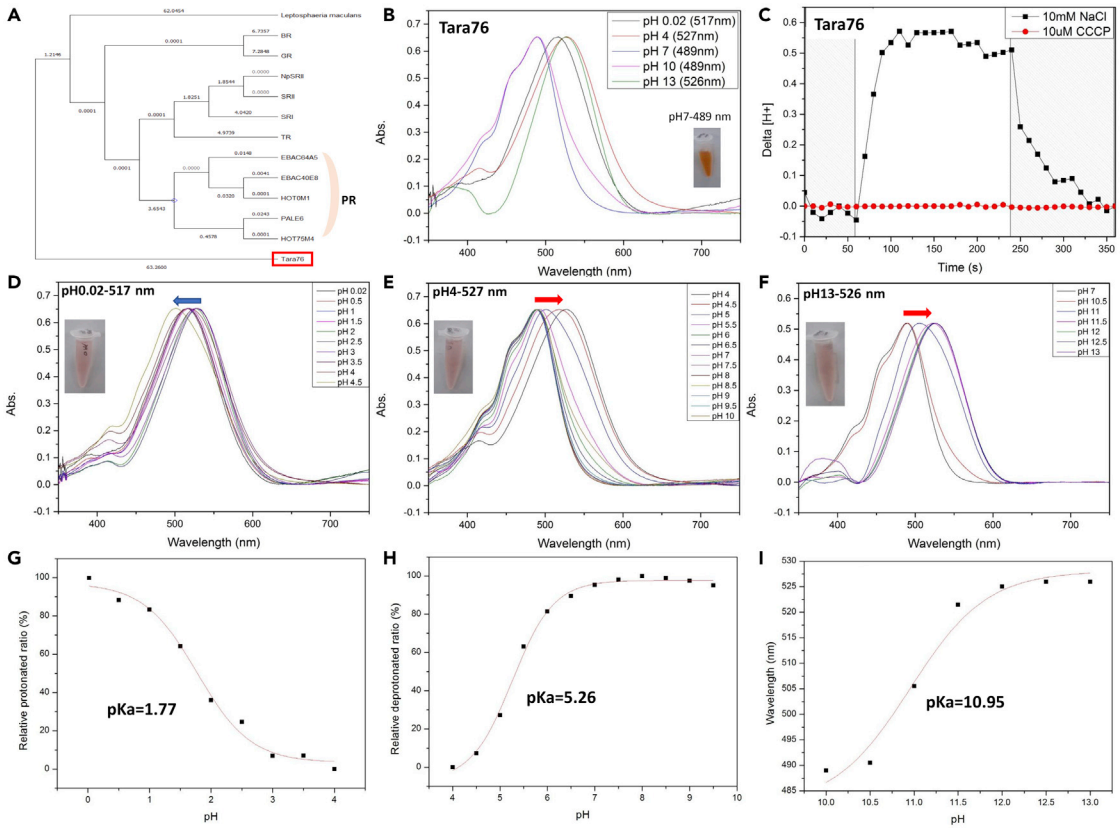

Figure 1. Phylogenetic tree and photochemical analysis of Tara76 rhodopsin

(A) The evolutionary history was inferred using the maximum likelihood method based on the Jones-Taylor-Thornto matrix-based model. Evolutionary analyses were conducted in MEGA7 (Jones et al., 1992; Kumar et al., 2016). The red squares are Tara76 rhodopsin, and the PRs are shown in a group.

(B) The absorption spectra of Tara76 rhodopsin at pH 0.02, 4, 7, 10, and 13, and orange color of Tara76 rhodopsin at neutral pH.

(C) The proton outward pumping was measured. The black dotted line was measured in an unbuffered solution of 10 mM NaCl, and the red dotted line was the result of treatment with 10 mM NaCl and 10 uM CCCP (carbonyl cyanide m-chlorophenylhydrazone). The gray area is dark, and the white area is in the presence of light for 3 min at 25°C.

(D–F) The absorption spectra were measured depending on pH changes. The red-shifted (red arrow) and blue-shifted (blue arrow) absorption spectra at each pH are indicated by arrows, and purified rhodopsins are exhibited at their representative pH. Panels D, E, and F represented at pH 0.02, 4, and 13.

(G–I) The pH titration curve for the calculation of pKa. Equation 'y = A/1+(pH 10-pKa)' was applied to fit the data using Origin Pro 7.0 where A is the maximal amplitude of relative absorbance changes (Zhu et al., 2013). Panels G, H, and I represented the measurements performed at pH range 0 to 4, 4 to 10, and 10 to 13.

pH resistance

Tara76 rhodopsin exhibited a typical absorbance spectrum under extreme pH conditions (Figures 1D and 1F). The pH resistance of Tara76 rhodopsin was tested with decreasing absorbance of the pigment at extremely acidic pH. At pH 0.02, Tara76 rhodopsin did not present any changes in absorbance for more than 30 days (Figure 2A). This confirmed that the maximum absorption value does not change since rhodopsin has retinal as a chromophore, and it does not aggregate or denature due to extreme pH.

To compare the stability of these pH changes, GR, PR, and TR were also tested. We measured the change in the ratio of the protein to the aggregation or denaturation through the change in pH. All the samples were measured at pH 7 as a maximum ratio of 1. Tara76 rhodopsin had stronger pH resistance than other microbial rhodopsins, and PR, GR, and TR exhibited very low stability at pH < 2. However, Tara76 rhodopsin exhibited stability at pH < 0.7 (Figure 2B). In the alkaline condition (≥pH 10), GR, PR, and TR presented a rapid decrease in absorbance. These proteins were not stable at pH > 11. However, Tara76 rhodopsin exhibited more than 70% stability at pH 12 and pH resistance by more than 50% of total protein at pH 13.

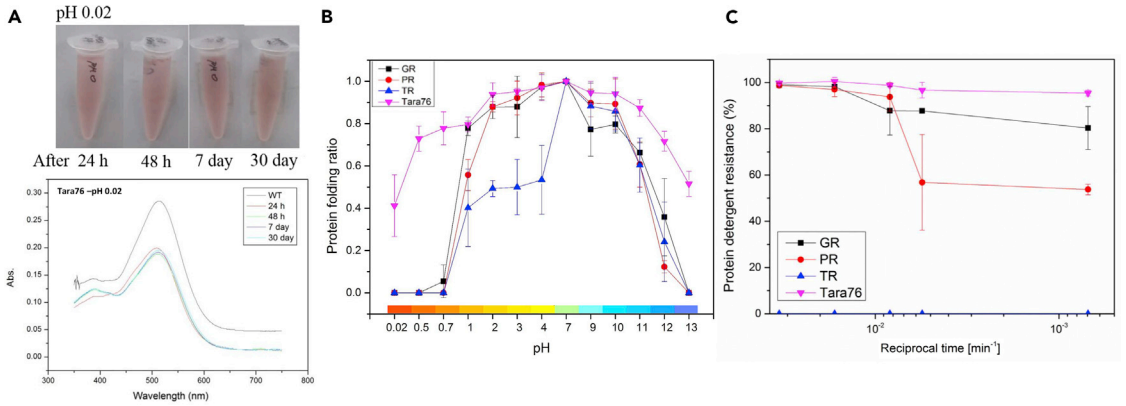

Figure 2. pH resistance test and detergent resistance test

(A) The stability was tested for 30 days at pH 0.02. Even under extreme acidic conditions, Tara76 rhodopsin retained a colored pigment for more than 1 month

(B) pH-dependent absorption spectra showing how stable each rhodopsin was at each pH. The Y axis was calculated as the ratio between colored and denatured protein at 25°C. In comparison, GR (black square line), PR (red circle line), TR (blue triangle line), and Tara76 rhodopsin (pink reverse triangle line) were measured.

(C) The resistance of GR, PR, TR, and Tara76 rhodopsin to Triton X-100 was measured. Each protein was solubilized by Triton X-100, and the maximum absorption spectra were measured over time. The temperature was maintained at room temperature and measured for 1,440 min (one day) starting at 0 min for 30 min after treatment for solubilization. The error bars are the standard deviations of three independent experiments (n = 3). GR, PR, TR, and Tara76 rhodopsin are designated as black, red, blue, and pink, respectively.

In addition, Tara76 rhodopsin exhibited ~80% activity at pH 0.5 and ~50% activity at pH 0.02. Thus, Tara76 rhodopsin had strong resistance to extreme pH, a sensitive physical condition. In addition, when the pH increased from pH 0.02 to 4, the absorption spectrum was almost restored to the absorption spectrum at pH 4. Tara76 rhodopsin was stable for at least 30 days at pH 0.02. In contrast, both GR and PR exhibited maximum absorption and color for only one day, and TR exhibited low stability at low pH (Figure S4). The stability at each extremely acidic and alkalic pH was measured in time-dependent manner (Figure S5). The TR showed very low stability at pH < 4, pH > 10, and PR, GR also showed low stability but they were a little bit more stable than TR. The Tara76 rhodopsin has been shown to have long-lasting stability at various pH values. Comparative experiments were performed to confirm the stability of Tara76 rhodopsin with GR, PR, and TR.

Detergent resistance

The detergent resistance of *Leptosphaeria* rhodopsin has been reported (Ji et al., 2017). To test the detergent solubility of Tara76 rhodopsin, the absorption spectra of SDS and Triton X-100 were compared based on DDM solubilization (Figure S6). The detergent resistance was measured in a time-dependent manner. After detergent treatment, the solubilization process was carried out every 30 min, and the insoluble protein was removed. After the solubilization of Tara76 rhodopsin in Triton X-100 or SDS, the protein was ~95% and 48% stable, respectively. Triton X-100 solubilization exhibited a spectrum similar to the absorption spectra in DDM, but SDS had a slightly broader spectrum. The Triton X-100 as a strong detergent was stabilized in a form similar to solubilization with DDM. Tara76 rhodopsin was stable in Triton X-100 but was slightly unstable in SDS. Although SDS is a strong anionic detergent that affects hydrophobicity, the Tara76 rhodopsin structure is very stable due to strong hydrophobic helix interactions inside the membrane.

The resistance to various detergents was compared to that of GR, PR, and TR (Figure 2C). The extent of solubilization by each detergent was lower for these three rhodopsins than for Tara76 rhodopsin. A solubilization test was performed in which a sample was treated with the detergent for 30 min, and the unfolded protein was removed. Each sample was measured every hour for one day. In the case of Tara76 rhodopsin, it was consistently stable in the detergent. However, regardless of the solubilization time, TR entered the unfolding state and lost the pigment color. PR stability decreased rapidly 2 h after mixing, but it retained ~50% activity after 24 hr. GR exhibited ~80% stability even after 24 hr; thus, the detergent resistance was relatively higher than the pH and vide infra.

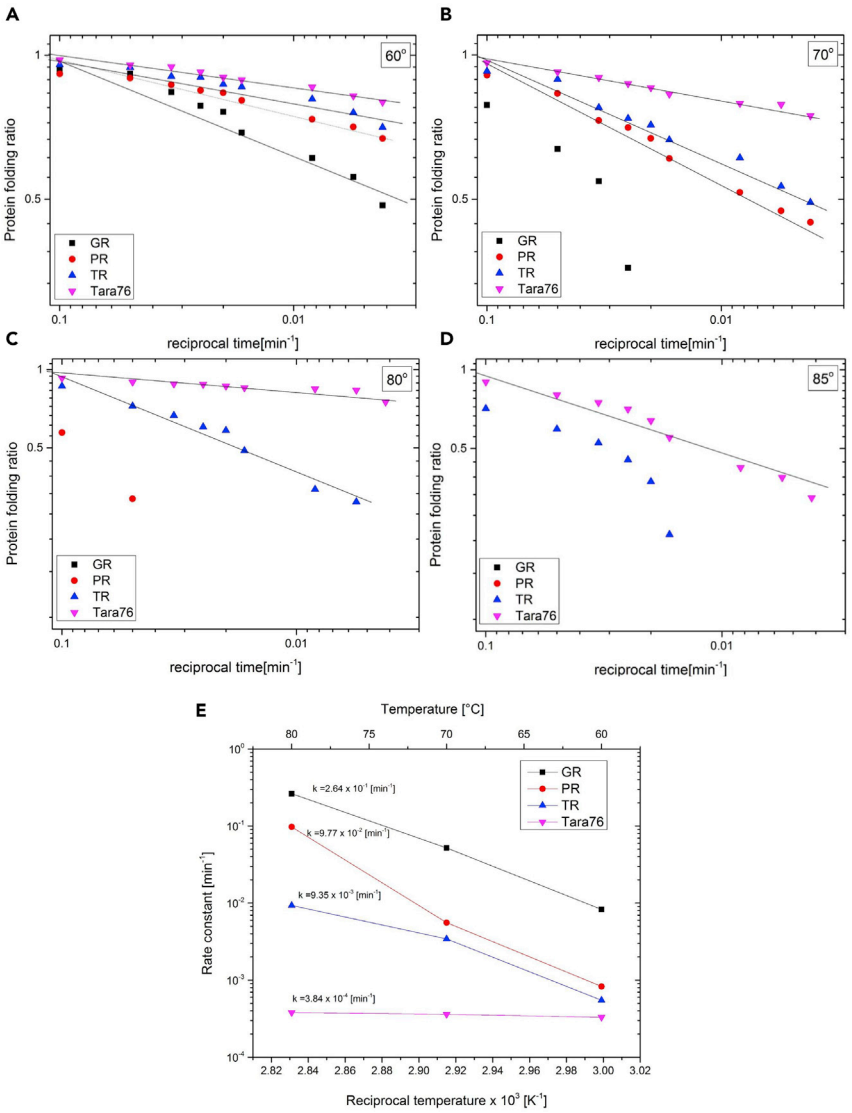

Figure 3. Thermal stability and denaturation curve

(A–D) Protein denaturation curves were plotted with temperature changes. GR, PR, TR, and Tara76 rhodopsin were tested at 60°C, 70°C, 80°C, and 85°C, respectively. The black square line represents GR, the red circle line represents PR, the blue triangle line represents TR, and the pink reverse triangle line represents Tara76 rhodopsin. The starting point was measured at room temperature every 10 min for 1 hr and then every 60 min for 240 min at each temperature. The unit of the Y axis is the protein folding ratio (%), which is the rate that the retinal is bleached from the rhodopsin, rendering the pigments colorless. The unit of the X axis is reciprocal time [min^{-1}].

(E) The denaturation rate constant (k0.5) was determined from each sample data from temperature. The values are calculated at 80°C, and the values of 60°C and 70°C are shown in Table S1. The unit of the X axis is reciprocal temperature [K^{-1}].

Thermal stability

TR has already been reported to be stable up to 75°C and RxR up to 85°C for 10 hr (Kanehara et al., 2017; Tsukamoto et al., 2013). Identifying thermal stability is an important factor for application in biochips and biosensors. Tara76 rhodopsin exhibited strong stability at 80°C and 85°C (Figures 3C and 3E). To compare these findings, we measured the outward proton-pumping activity and thermal stability as with TR (Figure 3).

The denaturation rate constant (*k0.5*) was compared for numerical analysis (Figure 3E). At 60°C, the *k0.5* values of PR, TR, and Tara76 rhodopsin were similar. At 70°C, PR and TR had similar *k0.5* values, whereas Tara76 rhodopsin

seemed to have a lower *k0.5* value than the other samples and a similar value at 60°C. This shows sufficient stability even at 70°C. At 80°C, PR had a *k0.5* value of 9.77×10^{-2} and TR 9.35×10^{-3}, which is approximately 10 times more stable than PR. In the case of Tara76 rhodopsin, the value was 3.8×10^{-4}, which is not significantly different from 60°C to 70°C, and shows strong stability, approximately 23 times greater than that of TR. This confirmed that the stability of Tara76 rhodopsin at 60°C is similar to the stability at 80°C.

At 60°C, the stability of this rhodopsin was tested against GR. PR and TR were similar and had stable results up to 70°C. In the case of GR, the stability was maintained at approximately 30% at 60°C after 4 hr (Figure 3A). However, PR, TR, and Tara76 rhodopsin were stable at 60°C. At 70°C, GR quickly unfolded within 50 min, whereas PR and TR exhibited approximately 40% stability at 240 min. Tara76 rhodopsin exhibited strong stability at 70°C. At the extreme temperature of 80°C, GR and PR exhibited a rapid decrease and TR was 0% at 240 min. The stability of Tara76 rhodopsin was approximately 70% at 80°C until 240 min (Figure 3C). This confirmed higher thermal stability than that reported for TR. Tara76 rhodopsin was still ~40% stable at 85°C for 240 min (Figure 3D). TR decreased at 120 min to less than 10%, indicating that Tara76 rhodopsin was more stable than other microbial rhodopsins. Therefore, Tara76 rhodopsin exhibited not only pH stability but also high temperature stability. These results showed that Tara76 rhodopsin had high detergent resistance and high thermal and extreme pH resistance.

Stability of Tara76 rhodopsin under dual and triple conditions

Stability for one factor does not easily represent stability in a complex environment. Therefore, we combined conditions and tested the stability of microbial rhodopsins under complex conditions.

Thermal stability at various pH values

To measure the thermal and pH stability together, each temperature was measured for each pH range for 240 min. In the acidic condition, the thermal stability decreased with declining pH. The stability was maintained at 60°C until pH 3, and Tara76 rhodopsin was more stable at pH 3 than pH 4 at 70°C. In the case of 80°C, the stability decreased as the pH decreased. In addition, at 60°C and pH < 3, the stability decreased as the pH decreased. At 70°C, the protein was relatively stable at low pH, as seen in the case of pH 3 and 4. At 80°C and pH < 3, the stability decreased as the pH decreased. As the temperature increased, pH 5 to 7 decreased protein stability but pH 3 to 4 resulted in strong stability. At pH 7 to 11, strong stability was measured regardless of temperature. At pH < 3 and pH > 12, the stability slightly decreased with temperature.

At pH 7, the protein was stable under all conditions. The deprotonation of the Schiff base of Tara76 rhodopsin was affected by high pH values. At pH ≥ 11, the stability was relatively decreased at each temperature. At 60°C and 70°C, Tara76 rhodopsin exhibited stability at pH 11 but kept decreasing up to 80°C. At pH 12, the overall stability was slightly reduced at all temperatures. At pH 13, almost all rhodopsins were not stable at 60°C for 30 min, and the stability decreased sharply at other temperatures. Thus, pH-dependent thermal stability of Tara76 rhodopsin was broadly stable under dual conditions.

The protein stability of Tara76 rhodopsin at each temperature and pH is shown in a 3D color map (Figure 4A). Tara76 rhodopsin was stable at 60°C, 70°C, and 80°C at pH 7 and had strong stability even under extreme alkaline conditions. From pH 7 to 10, the protein had strong stability up to 80°C. Tara76 rhodopsin was relatively stable at 60°C and 70°C at pH 12 but had low stability at 80°C. This suggests that Tara76 rhodopsin has stability under extreme alkaline conditions and is affected by the protonation state of the proton acceptor. To confirm these findings, the acceptor residue D78 (D85 standard in BR) of Tara76 rhodopsin was replaced with asparagine. In the protonated state, the Tara76 rhodopsin D78N mutant exhibited greater stability than WT. The thermal stability was also tested for the Tara76 rhodopsin D78N mutant at 85°C (Figures S7 and S8).

In the experiment at 85°C, TR exhibited near 0% stability at 120 min. In the case of Tara76 rhodopsin, the stability was ~20% up to 600 min, and the thermal stability was higher than that of TR. The Tara76 rhodopsin D78N mutant showed approximately 70% stability at 85°C until 600 min. Thus, the Tara76 rhodopsin D78N mutant had strong stability even in extreme high-temperature environments. This confirmed that the protein stability was affected by the protonation state.

Detergent stability at various pH values

To confirm the stability in detergent and pH resistance as another dual condition, the experiment with Triton X-100 showed strong stability of Tara76 rhodopsin. The solubilization of GR, PR, TR, and Tara76

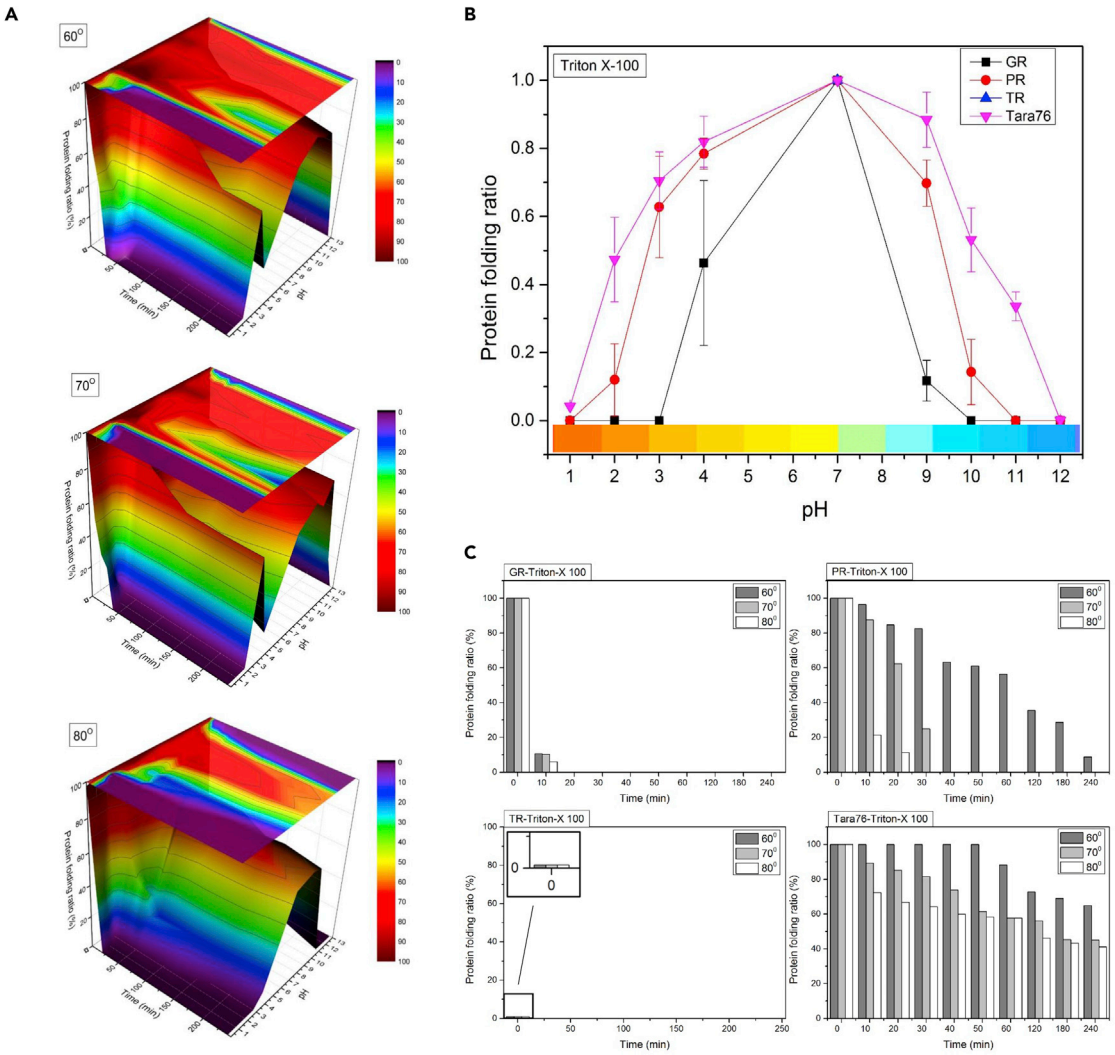

Figure 4. Dual conditions for the stability of Tara76 rhodopsin

(A) Thermal stability at various pH values. 3D color map surface that measured the stability of Tara76 rhodopsin with the pH, from pH 0.14 to pH 13 at each temperature from 0 to 240 min. The Y axis calculated the protein folding ratio (%) that the sample color was maintained at each temperature condition: it is 0% in purple color and 100% in red color.

(B) Detergent stability under acidic and alkaline pH conditions. Combined result of pH resistance to strong detergent. Protein folding ratio of each sample solubilized with 1% Triton X-100 (final concentration) was plotted according to pH at 25°C. GR is a black square, PR is a red circle, TR is a blue triangle, and Tara76 rhodopsin is a pink reverse triangle. In the case of TR, the detergent resistance was low, and low resistance was observed according to pH. The error bars are the standard deviations of three independent experiments (n = 3).

(C) Thermal stability with detergent resistance. The bar graph confirmed the stability of each temperature in the detergent condition. The temperature stability of GR, PR, TR, and Tara76 rhodopsin was observed after solubilization using strong detergent Triton X-100 (1% final con.). The low values of the figure were enlarged as black line boxes. The protein folding ratios were obtained by maximum absorption at 60°C, 70°C, and 80°C, respectively. Dark gray is at 60°C, medium gray is at 70°C, and light gray is at 80°C.

rhodopsin was performed at a final concentration of 1% Triton X-100 (Figure 4B). As shown in the previous results, TR did not exhibit detergent resistance and had low pH resistance under detergent stress conditions. GR and PR exhibited lower solubility than Tara76 rhodopsin.

The protein folding ratio was determined by the absorption spectra of each protein when changing from pH 7 to either acidic or alkaline pH. Like stable solubilization with DDM, Tara76 rhodopsin exhibited strong stability in each pH region with Triton X-100. PR exhibited strong resistance to pH and detergent compared to GR and TR (red circle in Figure 4B). In the case of GR, the resistance to pH was strong in DDM but

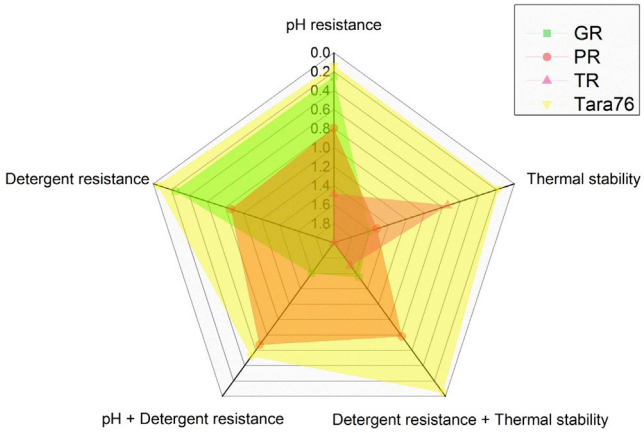

Figure 5. Five primal radar charts

The results of GR, PR, TR, and Tara76 rhodopsin are summarized. Each rhodopsin is shown radially, including pH resistance, detergent resistance, thermal stability, and dual condition. These values were obtained through the respective denaturation rate constants. The green color is GR, the red color is PR, the pink color is TR, and the yellow color is Tara76 rhodopsin.

relatively weak with the other detergents (black square in Figure 4B). PR was similar to GR but had a relatively high resistance to detergent and stability of ~60% at pH 3 and 9, with decreasing stability afterward. Tara76 rhodopsin had approximately 50% stability at pH 2 and 11, and it was stable somewhere outside that pH region (pink reverse triangle in Figure 4B). Thus, the pH resistance of Tara76 rhodopsin was strong according to the detergent.

Thermal stability with Triton X-100

Finally, thermal stability and detergent resistance were examined together to confirm stability under dual conditions. The stability of each sample according to detergent resistance in Triton X-100 was evaluated at 60°C, 70°C, and 80°C (Figure 4C). As mentioned above, GR, PR, and TR had low resistance to Triton X-100. However, for comparison with Tara76 rhodopsin, a small number of solubilized samples were collected and compared. In the case of TR, the detergent resistance was low, as was the thermal stability, consistent with previous results of low pH resistance under detergent stress. GR and PR had low solubility, and GR had relatively weak stability under dual conditions of detergent and pH.

As with TR, GR did not exhibit thermal stability with solubilization in Triton X-100. PR was relatively stable at 60°C, 70°C, and 80°C but exhibited a continuous decrease of approximately 10% stability at 60°C for up to 240 min. At 70°C and 80°C, the stability was almost 0% at approximately 30 min. However, Tara76 rhodopsin exhibited strong stability under the dual condition. At 60°C, stability was 100% for up to 50 min and then slightly decreased. At 70°C and 80°C, the stability was ~50% up to 180 min, and the thermal stability was relatively strong (45%) at 240 min.

Stability under the intersection of double conditions

After confirming the stability of Tara76 rhodopsin under dual conditions, we evaluated the stability under all three conditions. The stability of Tara76 rhodopsin under the individual and dual conditions was combined with radar data (Figure 5) and summarized by obtaining the denaturation rate constant under the indicated conditions. Tara76 rhodopsin was clearly stable as in the previous results.

Extreme environmental resistance for bio-electrical applications

Microbial rhodopsins are candidates not only for optogenetic tools but also for electrobiological applications such as biochips or biosensors. We attempted to confirm the stability of the protein at high salt concentrations and during regeneration after dehydration stress through heat. High salt concentrations generally affect the stability of proteins through electrostatic effects, which limit electrobiological applications.

We confirmed the stability of Tara76 rhodopsin compared to GR, PR, and TR under high salt conditions (Figure 6A). Stability was reduced with 4 M sodium chloride compared to the stable environment. The

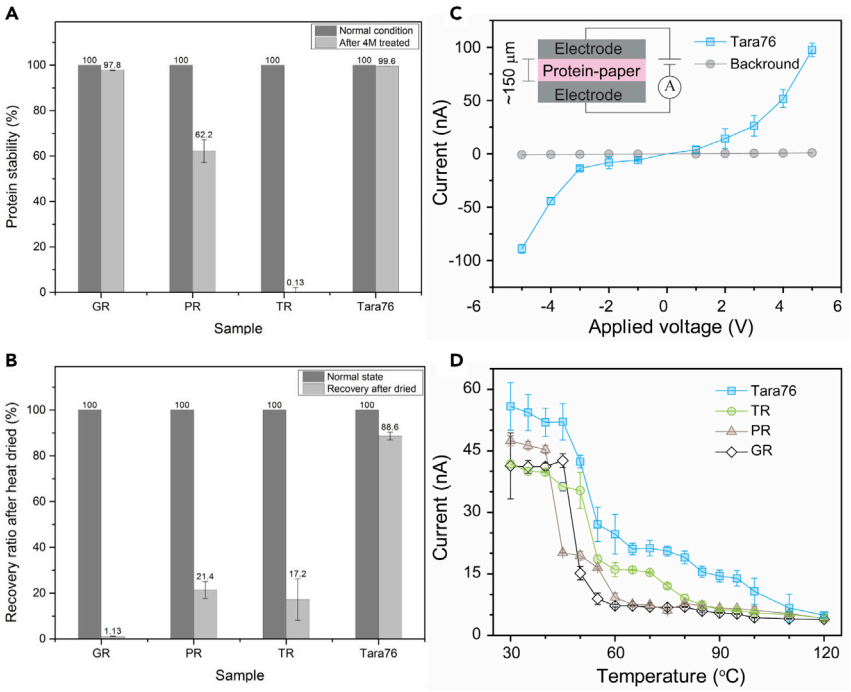

Figure 6. Comparison of stability under high salt conditions and recovery after heat drying and electrical conductivity of proteins (Tara76 rhodopsin, TR, PR, and GR)

(A) Protein stability of GR, PR, TR, and Tara76 rhodopsin is confirmed at high concentrations of 4 M sodium chloride. The measurements were made after 24 hr of treatment. The dark bar graph is under the normal condition, and the light gray bar is at the high salt concentration. These are shown as a ratio

(B–D) (B) Each sample was dried for 16 hr at 55°C. The dark bar graph shows the state before drying, and the light gray bar shows that the color remained after recovery in 0.02% DDM solution. The error bars are the standard deviations of three independent experiments (n = 3). Electrical current flow through the proteins in the paper matrix during (C) various voltages and (D) various temperatures and 4-volt were applied. The inset of (C) is a setup for current measurement.

24-h absorption spectra are shown in Figure S9. GR was stable under the high salt conditions with a decrease of ~3%. However, PR stability was reduced by approximately 40% and TR stability by 99%. In contrast, Tara76 rhodopsin presented almost no loss, retaining 99.6% stability.

We also tested the stability for thermal drying. Drying was carried out at 55°C for 24 hr to study stability after dehydration. The ratio of the recovered microbial rhodopsin was calculated by the λmax of the absorption spectrum after recovering from 0.02% DDM treatment (Figure 6B). We measured optical density (OD) at the wavelength of maximum absorption peak after recovery for the dehydration effect of rhodopsin proteins. Previously, we checked and compare the OD at maximum peak and the area of absorbance. They were very similar values, and either of them can used for the protein amount for the rhodopsin (Tsogbadrakh et al., 2018).

In the case of GR, we found that the dehydrated protein lost absorption. In contrast, PR and TR recovered 21% and 17%, respectively. However, Tara76 rhodopsin was restored to 89%. The stability of Tara76 rhodopsin to dehydration and the maintenance of the chromophore are shown in the absorption spectra of the restored protein (Figure S10). The chromophore was bright violet after dehydration and changed back to its original color after restoration (Figure S10D).

Since a protein can conduct electricity both in dry and wet states, it has the potential to be used as semiconductors for electronic devices (Evans and Gergely, 1949; Rosenberg, 1962). High-temperature stable proteins have been demanded to be tested in electronic applications. To study the electrical property of our protein (Tara76 rhodopsin) compared to TR, PR, and GR, we measured electrical current flow through multilayers of these proteins after they were dried and incubated at various temperature from 30°C to

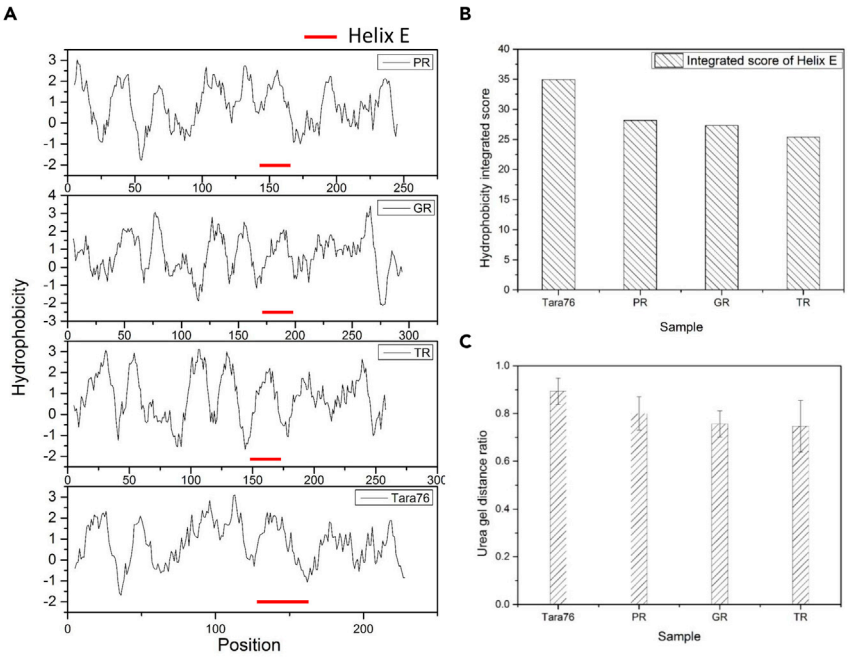

Figure 7. Hydrophobicity analysis of helix E

The hydrophobicity of Tara76 rhodopsin was compared with that of GR, PR, and TR.

(A) The hydrophobicity score of all amino acids is shown in helix E. The numerical value of the amino acid was determined through ProtScale from ExPAsy, and the helix E portion of each protein was indicated by a red line. In the case of Tara76 rhodopsin, from the 129th residue to the 152nd residue, PR indicates 147th to 170th residue, GR indicates 174th to 197th, and TR indicates 148th to 17.

(B) The hydrophobicity score of the helix E region was added and compared with the bar graph.

(C) The urea gradient gel analysis, which is the result of hydrophobicity depending on how far the protein migrates through transverse urea gradient gel electrophoresis (TUG-GE). The concentration is 0 M at the top and 8 M at the bottom. Since it forms a continuous concentration, the stability of the protein depending on the concentration can be seen. This is expressed as a ratio according to the distance moved away. The error bars are the standard deviations of three independent experiments (n = 3).

125°C. The I-V curve shows that electrical current passed through the multiplayer of the protein that was immobilized in the paper matrix (Figures 6C and 6C inset). The electrical current flow of Tara76 rhodopsin was higher than that of GR, PR, and TR at room temperature (Figure 6D). In the case of GR and PR, the current flow almost disappeared at temperatures exceeding 50°C. Tara76 rhodopsin exhibited high conductivity at high temperatures, with a current of 10 nA at 100°C. We also confirmed the thermal stability with current flow observed at temperatures exceeding 100°C. Tara76 rhodopsin exhibited strong stability to temperature and dehydration stress compared to the other samples and high electric current flow efficiency. Thus, Tara76 rhodopsin can be highly utilized under various conditions.

Hydrophobicity of Tara76 rhodopsin helix E

Questioning the reason for the strong stability of Tara76 rhodopsin, we considered the effects of hydrophobicity on protein stability (Pace et al., 2014, 2011; Van den Burg et al., 1994), particularly the hydrophobic amino acids of the helix. The hydropathy analysis of each rhodopsin and each helix was made by TCDB WHAT 2.0 analysis (Figure 7A) (Saier et al., 2006). The hydrophobicity of the helix E portion of Tara76 rhodopsin was relatively higher than that of other rhodopsins. The hydrophobicity score for each rhodopsin was compared to the hydropathicity amino acid scale using ProtScale of ExPASy (Gasteiger et al., 2005; Kyte and Doolittle, 1982). The hydrophobicity score of helix E was 20, ~30% higher than the hydrophobicity score of GR, PR, or TR (Figure 7B). To study the effect of the hydrophobic effects on helix E, the helix E portion of Tara76 rhodopsin was substituted with PR. The 129th residue to the 152th residue of Tara76 rhodopsin was replaced with the 147th to 170th amino acids that are a part of the helix E of PR. The helix E of PR showed a low hydrophobicity score of about 23% by comparing the Tara76 rhodopsin

hydrophobicity score (Figure S11D). The chimeric Tara76 rhodopsin was well expressed and showed the proton-pumping activity (Figures S11A and S11B). The hydrophobicity contributes to protein stability, and a comparative experiment was performed through thermal stability (Figure S11C). The chimeric Tara76 rhodopsin showed a significant decrease in high-temperature stability compared with Tara76 rhodopsin WT. Through this, it suggests that the hydrophobicity of helix E contributes to the protein stability.

To confirm that the hydrophobicity of helix E of Tara76 rhodopsin affects the stability of the protein, we used a urea continuous environment in transverse urea gradient gel electrophoresis (TUG-GE). This showed the hydrophobicity of the whole protein (Figure 7C). The ratio of protein movement was calculated with the total length set to 1. Tara76 rhodopsin had the highest value that was farthest from the starting point. Thus, the high hydrophobicity of Tara76 rhodopsin may affect stability.

DISCUSSION

The stability of microbial rhodopsins was tested by considering several factors, including temperature, pH, detergent, high salt concentration, and dehydration. This stable protein was extracted from microorganisms living in extreme environments (Ece et al., 2015; Ji et al., 2017; Otzen, 2002; Shionoya et al., 2018), and the results led to continued research on various applications such as biochips and biosensors, as well as optogenetic tools (Li et al., 2018). In this study, we investigated Tara76 rhodopsin, which exhibits stability against temperature, detergent, pH, salt, and dehydration. Tara76 rhodopsin exhibited strong stability even under dual and triple conditions.

Since Tara76 rhodopsin was stable under extreme pH conditions while measuring absorption spectra for each pH to analyze its photochemical characteristics, various factors also were studied. Comparing each denaturation rate constant (Figure 5), the pH resistance of Tara76 rhodopsin was twice that of GR, and it had a denaturation rate constant six times lower than that of PR and 10 times lower than that of TR. Therefore, the stability of Tara76 rhodopsin is much higher than the stability of these other rhodopsins. In the case of Tara76 rhodopsin, the *k0.5* value was 10 times lower than that of PR and TR and five times lower than that of GR. Under the dual condition of pH and detergent, Tara76 rhodopsin was 1.2 times more stable than PR and twice as stable as GR. In the other dual condition for detergent and temperature, Tara76 rhodopsin was stable, with a *k0.5* value 16 times lower than that of PR and 31 times lower than that of GR. These values indicate that Tara76 rhodopsin had relatively high stability under various conditions.

Tara76 rhodopsin stability at various temperatures and under the dual pH and temperature condition was tested at high pH (i.e., pH 10 and 11). Comparing the results with the D78N mutant suggested that microbial rhodopsins are more stable when the proton acceptor residue is in the protonated state. The protonated counter ion reduces the energy gap between the electronic ground and the excited state (Kanehara et al., 2017). When protonation occurs, the energy gap is reduced, which has structural stability compared to a protein in a relatively normal state. Since the D78N mutant maintains protonation, it can be resistant to the stability of the protein itself even at extreme temperatures. However, at low pHs (2, 3, & 4) Tara76 rhodopsin showed relatively low stability at the temperatures (Figure 4A), because the proton acceptor of Tara76 rhodopsin was deprotonated at pH 2, 3, & 4. Due to this, it showed instability in high temperature at low pH 2, 3, and 4. The stability was maintained even at extreme temperatures since it exists in a more stable form than the protonated state due to the increased hydrophobicity.

The gene of this study, Tara76 opsin, is obtained from Tara Oceans Expedition. The sequence information was extracted from an uncultured bacterium, and the gene discovered through this project was in large quantities to form a library. It was found in the southeastern Mediterranean Sea. Since it was a mixed sample, the environment was estimated to be a mixed layer depth of approximately 50 m and a mixed layer ranging from 23°C to 23.5°C (Dubinsky et al., 2017). Also, the salinity is estimated to be approximately 39 PSU. Since this location is an upper mixed layer in the sea, it needs to respond to various conditions. In general, rhodopsin must adapt to an extreme environment. These membrane proteins are the first to encounter the external environment. Therefore, the cell needs to increase its resistance to the environment by enhancing the stability of the protein itself rather than defending through various regulatory mechanisms. However, the cause for such stability remains questionable. We used the hydrophobicity of the protein to examine the cause of stability. The thermal stability of the substituted chimeric Tara76 rhodopsin decreased significantly. The hydrophobicity of helix E compared to the whole protein indicated that the

hydrophobicity score of Tara76 rhodopsin was somewhat higher than that of GR, PR, and TR. TUG-GE confirmed the hydrophobicity of Tara76 rhodopsin through a gradient gel using urea in an sodium dodecyl sulfate-polyacrylamide-gel electrophoresis system (Gianazza et al., 1998; Goldenberg, 2001), approaching the concentration of 8M urea. To explain the hydrophobic effect on the stability of Tara76 rhodopsin, we replaced the helix E part with helix of PR that has a low hydrophobicity score of about 23% compared with Tara76 rhodopsin. We performed the expression and purification, and the proton-pumping activity was also tested. The thermal stability was measured and shown that Tara76 rhodopsin lost its stable properties at high temperatures. This chimeric Tara76 rhodopsin lost its chromophore within 1 hr at 85°C (Figure S11C). These results indicate that the hydrophobic property of Tara76 rhodopsin is high and the hydrophobic state of helix E may contribute to the stability of Tara76 rhodopsin. The hydrophobicity of these proteins is related to protein stability, which is also related to the stability of Tara76 rhodopsin. It reported that the stability of SDS detergent was influenced by hydrophobicity (Honda et al., 2017). In this study, it was also shown that the hydrophobicity of Tara76 rhodopsin contributes significantly to the protein stability, which is suggested by the above results. The thermal stability is influenced by the strength of physicochemical interactions within the protein. It suggested that the hydrophobicity of amino acids that forms retinal chromophore is high, and this hydrophobicity cluster contributes to structural stability. In this study, the physicochemical interaction effect of Tara76 rhodopsin on hydrophobicity is also shown to be a major factor. The stability of the Tara76 rhodopsin for mechanical and engineering applications was confirmed for several factors. We tested the stability at a high concentration of sodium chloride, as high concentrations of ions affect the electrostatic attraction of proteins. Tara76 rhodopsin was >99% stable even under the 4 M sodium chloride condition. Tara76 rhodopsin was also very stable after dehydration at 55°C for 24 hr, recovering by ~89%. In contrast, TR and PR recovered only about 20%, and GR had the weakest stability. When Tara76 rhodopsin was dehydrated, the λmax red shifted to reddish purple and returned to its original wavelength after recovering. These shifts show that the protein structure is modified under extreme conditions but restored under stable conditions. Thus, the recovery and tolerance of Tara76 rhodopsin itself are excellent.

Based on our study of the stability of Tara76 rhodopsin under a variety of conditions, we also tested its basic physical properties for mechanical and engineering applications. In a test of the electrical current flow through protein immobilized on the paper matrix, the changes in current were measured by increasing the temperature from 30°C to 120°C. We measured strong stability and high current flow efficiency. The tendency for protein current flow from room temperature to 50°C was different from that at 50°C or higher and again at ~80°C, indicating that the protein may have three forms depending on the temperature. In addition, we again confirmed the protein's stability at high temperatures. Therefore, Tara76 rhodopsin may benefit bioengineering applications. A structural approach is needed to study the stability of Tara76 rhodopsin to identify and develop the function of Tara76 rhodopsin's pumping activity under the various conditions. We are pursuing further research on its stability and applications under various conditions.

SUPPLEMENTAL INFORMATION

Supplemental information can be found online at https://doi.org/10.1016/j.isci.2021.102620.

STAR★METHOD

Detailed methods are provided in the online version of this paper and include the following:

- KEY RESOURCES TABLE
- RESOURCE AVAILABILITY
  - Lead contact
  - Materials availability
  - Data and code availability
- METHOD DETAILS
  - DNA cloning and expression
  - Protein purification
  - Absorption spectroscopy at various pH and pKa values
  - Proton pump assay
  - Thermal stability measurements
  - pH resistance measurements

- Detergent resistance measurements
- Transverse urea gradient gel electrophoresis (TUG-GE)
- Measurement of electric current

- QUANTIFICATION AND STATISTICAL ANALYSIS
  - Progress under each condition for protein stability experiments
  - Protein stability measurement over time
  - Accession numbers

ACKNOWLEDGMENTS

This work was supported by the Samsung Science and Technology Foundation, South Korea under Project Number SSTF-BA1801-06. We thank Professor Oded Beja for providing initial sequence information and fruitful discussion.

AUTHOR CONTRIBUTIONS

J.G.S. and K.H.J. conceived and performed the experiments, wrote the manuscript, and secured funding. V.S., K.W.K., K.C., S.G.C., J.H.K., and S.M. performed the experiments. A.P. and K.S. provided expertise and feedback.

DECLARATION OF INTERESTS

The authors declare no competing interests.

Received: February 22, 2021
Revised: April 28, 2021
Accepted: May 19, 2021
Published: June 25, 2021

REFERENCES

Béjà, O., Aravind, L., Koonin, E.V., Suzuki, M.T., Hadd, A., Nguyen, L.P., Jovanovich, S.B., Gates, C.M., Feldman, R.A., Spudich, J.L., et al. (2000). Bacterial rhodopsin: evidence for a new type of phototrophy in the sea. Science *289*, 1902–1906.

Dubinsky, V., Haber, M., Burgsdorf, I., Saurav, K., Lehahn, Y., Malik, A., Sher, D., Aharonovich, D., and Steindler, L. (2017). Metagenomic analysis reveals unusually high incidence of proteorhodopsin genes in the ultraoligotrophic Eastern Mediterranean Sea. Environ. Microbiol. *19*, 1077–1090. https://doi.org/10.1111/1462-2920.13624.

Ece, S., Evran, S., Janda, J.-O., Merkl, R., and Sterner, R. (2015). Improving thermal and detergent stability of Bacillus stearothermophilus neopullulanase by rational enzyme design. Protein Eng. Des. Sel. *28*, 147–151. https://doi.org/10.1093/protein/gzv001.

Ernst, O.P., Lodowski, D.T., Elstner, M., Hegemann, P., Brown, L.S., and Kandori, H. (2014). Microbial and animal rhodopsins: structures, functions, and molecular mechanisms. Chem. Rev. *114*, 126–163. https://doi.org/10.1021/cr4003769.

Evans, M.G., and Gergely, J. (1949). A discussion of the possibility of bands of energy levels in proteins electronic interaction in non bonded systems. Biochim. Biophys. Acta *3*, 188–197. https://doi.org/10.1016/0006-3002(49)90091-8.

Finkel, O.M., Béjà, O., and Belkin, S. (2013). Global abundance of microbial rhodopsins. ISME J. *7*, 448–451. https://doi.org/10.1038/ismej.2012.112.

Foit, L., Morgan, G.J., Kern, M.J., Steimer, L.R., Hacht, A.A.von, Titchmarsh, J., Warriner, S.L., Radford, S.E., and Bardwell, J.C.A. (2009). Optimizing protein stability in vivo. Mol. Cell *36*, 861–871. https://doi.org/10.1016/j.molcel.2009.11.022.

Friedrich, T., Geibel, S., Kalmbach, R., Chizhov, I., Ataka, K., Heberle, J., Engelhard, M., and Bamberg, E. (2002). Proteorhodopsin is a light-driven proton pump with variable vectoriality. J. Mol. Biol. *321*, 821–838.

Gasteiger, E., Hoogland, C., Gattiker, A., Duvaud, S., Wilkins, M.R., Appel, R.D., and Bairoch, A. (2005). Protein identification and analysis tools on the ExPASy server. In The Proteomics Protocols Handbook, J.M. Walker, ed. (Humana Press), pp. 571–607. https://doi.org/10.1385/1-59259-890-0:571.

Gianazza, E., Eberini, I., Santi, O., and Vignati, M. (1998). Denaturant-gradient gel electrophoresis: technical aspects and practical applications. Analytica Chim. Acta *372*, 99–120. https://doi.org/10.1016/S0003-2670(98)00333-X.

Glock, C., Nagpal, J., and Gottschalk, A. (2015). Microbial rhodopsin optogenetic tools: application for analyses of synaptic transmission and of neuronal network activity in behavior. Methods Mol. Biol. *1327*, 87–103. https://doi.org/10.1007/978-1-4939-2842-2_8.

Goldenberg, D.P. (2001). Transverse urea-gradient gel electrophoresis. Curr. Protoc. Protein Sci. Chapter 7, Unit 7.4. https://doi.org/10.1002/0471140864.ps0704s03.

Govorunova, E.G., and Koppel, L.A. (2016). The road to optogenetics: microbial rhodopsins. Biochem. Mosc. *81*, 928–940. https://doi.org/10.1134/S0006297916090029.

Govorunova, E.G., Sineshchekov, O.A., Janz, R., Liu, X., and Spudich, J.L. (2015). Natural light-gated anion channels: a family of microbial rhodopsins for advanced optogenetics. Science *349*, 647–650. https://doi.org/10.1126/science.aaa7484.

Grote, M., Engelhard, M., and Hegemann, P. (2014). Of ion pumps, sensors and channels — perspectives on microbial rhodopsins between science and history. Biochim. Biophys. Acta *1837*, 533–545. https://doi.org/10.1016/j.bbabio.2013.08.006.

Hasemi, T., Kikukawa, T., Kamo, N., and Demura, M. (2016). Characterization of a cyanobacterial chloride-pumping rhodopsin and its conversion into a proton pump. J. Biol. Chem. *291*, 355–362. https://doi.org/10.1074/jbc.M115.688614.

Hirayama, J., Imamoto, Y., Shichida, Y., Kamo, N., Tomioka, H., and Yoshizawa, T. (1992). Photocycle of phoborhodopsin from haloalkaliphilic bacterium (Natronobacterium pharaonis) studied by low-temperature spectrophotometry. Biochemistry *31*, 2093–2098.

Honda, N., Tsukamoto, T., and Sudo, Y. (2017). Comparative evaluation of the stability of seven-transmembrane microbial rhodopsins to various physicochemical stimuli. Chem. Phys. Lett. *682*, 6–14. https://doi.org/10.1016/j.cplett.2017.05.055.

Hoque, M.R., Ishizuka, T., Inoue, K., Abe-Yoshizumi, R., Igarashi, H., Mishima, T., Kandori, H., and Yawo, H. (2016). A chimera Na+-Pump rhodopsin as an effective optogenetic silencer. PLoS One *11*, e0166820. https://doi.org/10.1371/journal.pone.0166820.

Inoue, K., Ito, S., Kato, Y., Nomura, Y., Shibata, M., Uchihashi, T., Tsunoda, S.P., and Kandori, H. (2016a). A natural light-driven inward proton pump. Nat. Commun. *7*, 13415. https://doi.org/10.1038/ncomms13415.

Inoue, K., Nomura, Y., and Kandori, H. (2016b). Asymmetric functional conversion of eubacterial light-driven ion pumps. J. Biol. Chem. *291*, 9883–9893. https://doi.org/10.1074/jbc.M116.716498.

Ji, L., Ma, B., Meng, Q., Li, L., Liu, K., and Chen, D. (2017). Detergent-resistant oligomeric Leptosphaeria rhodopsin is a promising bio-nanomaterial and an alternative to bacteriorhodopsin. Biochem. Biophys. Res. Commun. *493*, 352–357. https://doi.org/10.1016/j.bbrc.2017.09.018.

Jones, D.T., Taylor, W.R., and Thornton, J.M. (1992). The rapid generation of mutation data matrices from protein sequences. Comput. Appl. Biosci. *8*, 275–282.

Kanehara, K., Yoshizawa, S., Tsukamoto, T., and Sudo, Y. (2017). A phylogenetically distinctive and extremely heat stable light-driven proton pump from the eubacterium *Rubrobacter xylanophilus* DSM 9941^{T}. Sci. Rep. *7*, 44427. https://doi.org/10.1038/srep44427.

Kumar, S., Stecher, G., and Tamura, K. (2016). MEGA7: molecular evolutionary genetics analysis version 7.0 for bigger datasets. Mol. Biol. Evol. *33*, 1870–1874. https://doi.org/10.1093/molbev/msw054.

Kyte, J., and Doolittle, R.F. (1982). A simple method for displaying the hydropathic character of a protein. J. Mol. Biol. *157*, 105–132.

Li, Y.-T., Tian, Y., Tian, H., Tu, T., Gou, G.-Y., Wang, Q., Qiao, Y.-C., Yang, Y., and Ren, T.-L. (2018). A review on bacteriorhodopsin-based bioelectronic devices. Sensors (Basel) *18*. https://doi.org/10.3390/s18051368.

Magliery, T.J. (2015). Protein stability: computation, sequence statistics, and new experimental methods. Curr. Opin. Struct. Biol. *33*, 161–168. https://doi.org/10.1016/j.sbi.2015.09.002.

McIsaac, R.S., Bedbrook, C.N., and Arnold, F.H. (2015). Recent advances in engineering microbial rhodopsins for optogenetics. Curr. Opin. Struct. Biol. *33*, 8–15. https://doi.org/10.1016/j.sbi.2015.05.001.

Otzen, D.E. (2002). Protein unfolding in detergents: effect of micelle structure, ionic strength, pH, and temperature. Biophys. J. *83*, 2219–2230.

Pace, C.N., Fu, H., Fryar, K.L., Landua, J., Trevino, S.R., Shirley, B.A., Hendricks, M.M., Iimura, S., Gajiwala, K., Scholtz, J.M., and Grimsley, G.R. (2011). Contribution of hydrophobic interactions to protein stability. J. Mol. Biol. *408*, 514–528. https://doi.org/10.1016/j.jmb.2011.02.053.

Pace, C.N., Scholtz, J.M., and Grimsley, G.R. (2014). Forces stabilizing proteins. FEBS Lett. *588*, 2177–2184. https://doi.org/10.1016/j.febslet.2014.05.006.

Pushkarev, A., Hevroni, G., Roitman, S., Shim, J., Choi, A., Jung, K.-H., and Béjà, O. (2018a). The use of a chimeric rhodopsin vector for the detection of new proteorhodopsins based on color. Front. Microbiol. *9*. https://doi.org/10.3389/fmicb.2018.00439.

Pushkarev, A., Inoue, K., Larom, S., Flores-Uribe, J., Singh, M., Konno, M., Tomida, S., Ito, S., Nakamura, R., Tsunoda, S.P., et al. (2018b). A distinct abundant group of microbial rhodopsins discovered using functional metagenomics. Nature *558*, 595–599. https://doi.org/10.1038/s41586-018-0225-9.

Ranjan, P., and Kateriya, S. (2018). Localization and dimer stability of a newly identified microbial rhodopsin from a polar, non-motile green algae. BMC Res. Notes *11*, 65. https://doi.org/10.1186/s13104-018-3181-4.

Rosenberg, B. (1962). Electrical conductivity of proteins. Nature *193*, 364–365. https://doi.org/10.1038/193364a0.

Saier, M.H., Tran, C.V., and Barabote, R.D. (2006). TCDB: the Transporter Classification Database for membrane transport protein analyses and information. Nucleic Acids Res. *34*, D181–D186. https://doi.org/10.1093/nar/gkj001.

Schobert, B., and Lanyi, J.K. (1982). Halorhodopsin is a light-driven chloride pump. J. Biol. Chem. *257*, 10306–10313.

Shionoya, T., Mizuno, M., Tsukamoto, T., Ikeda, K., Seki, H., Kojima, K., Shibata, M., Kawamura, I., Sudo, Y., and Mizutani, Y. (2018). High thermal stability of oligomeric assemblies of thermophilic rhodopsin in a lipid environment. J. Phys. Chem. B *122*, 6945–6953. https://doi.org/10.1021/acs.jpcb.8b04894.

Spudich, J.L., and Luecke, H. (2002). Sensory rhodopsin II: functional insights from structure. Curr. Opin. Struct. Biol. *12*, 540–546. https://doi.org/10.1016/S0959-440X(02)00359-7.

Tsogbadrakh, O., Choi, A.R., and Jung, K.-H. (2018). Expression of Anabaena sensory rhodopsin is influenced by different codons of seven residues at the N-terminal region. Protein Expr. Purif. *151*, 1–8. https://doi.org/10.1016/j.pep.2018.05.011.

Tsukamoto, T., Inoue, K., Kandori, H., and Sudo, Y. (2013). Thermal and spectroscopic characterization of a proton pumping rhodopsin from an extreme thermophile. J. Biol. Chem. *288*, 21581–21592. https://doi.org/10.1074/jbc.M113.479394.

Tsukamoto, T., Mizutani, K., Hasegawa, T., Takahashi, M., Honda, N., Hashimoto, N., Shimono, K., Yamashita, K., Yamamoto, M., Miyauchi, S., et al. (2016). X-ray crystallographic structure of thermophilic rhodopsin: implications for high thermal stability and optogenetic function. J. Biol. Chem. *291*, 12223–12232. https://doi.org/10.1074/jbc.M116.719815.

Tsunoda, S.P., Sugiura, M., and Kandori, H. (2021). Molecular properties and optogenetic applications of enzymerhodopsins. Adv. Exp. Med. Biol. *1293*, 153–165. https://doi.org/10.1007/978-981-15-8763-4_9.

Van den Burg, B., Dijkstra, B.W., Vriend, G., Van der Vinne, B., Venema, G., and Eijsink, V.G. (1994). Protein stabilization by hydrophobic interactions at the surface. Eur. J. Biochem. *220*, 981–985.

Vogt, A., Guo, Y., Tsunoda, S.P., Kateriya, S., Elstner, M., and Hegemann, P. (2015). Conversion of a light-driven proton pump into a light-gated ion channel. Sci. Rep. *5*, 16450. https://doi.org/10.1038/srep16450.

Yoshida, K., Tsunoda, S.P., Brown, L.S., and Kandori, H. (2017). A unique choanoflagellate enzyme rhodopsin exhibits light-dependent cyclic nucleotide phosphodiesterase activity. J. Biol. Chem. *292*, 7531–7541. https://doi.org/10.1074/jbc.M117.775569.

Zhu, S., Brown, M.F., and Feller, S.E. (2013). Retinal conformation governs pKa of protonated Schiff base in rhodopsin activation. J. Am. Chem. Soc. *135*, 9391–9398. https://doi.org/10.1021/ja4002986.

STAR★METHOD

KEY RESOURCES TABLE

REAGENT or RESOURCE	SOURCE	IDENTIFIER
Bacterial and Virus Strains		
E. coli strain UT5600	NEB(new england biolabs)	Cat# E4129
Chemicals, Peptides, and Recombinant Proteins		
Carbonyl cyanide m-chlorophenylhydrazone 97%	Sigma-Aldrich	CAS#555-60-2
Deposited Data		
Gloeobacter rhodopsin	National Center for Biotechnology Information	GenBank accession no. WP_011140202.1
Proteorhodopsin	National Center for Biotechnology Information	GenBank accession no. Q9F7P4.1
thermal rhodopsin	National Center for Biotechnology Information	GenBank accession no. WP_014629850.1
Oligonucleotides		
Primer: Tara76- Forward: GCACGACTTCTTCAAGTCCGCCATGCC	This paper	N/A
Primer: Tara76- Reverse: AGGGCGGCCGCCTAGTGATGATGGTG GTGATGAGCAGTTGA	This paper	N/A
Software and Algorithms		
Origin.9.0	originlab	https://www.originlab.com/
Horiba data Navi program	horiba	https://horiba-data-navi.software.informer.com/

RESOURCE AVAILABILITY

Lead contact

Further information and requests for reagents may be directed to, and will be fulfilled by the corresponding author, Dr. Kwang-Hwan Jung (kjung@sogang.ac.kr).

Materials availability

All tables and figures are included in the text and supplemental information.

Data and code availability

The published article contains all data generated or analyzed.

METHOD DETAILS

DNA cloning and expression

Prof. Oded Béjà (Technion – Israel Institute of Technology, Israel) provided us with the DNA sequence of Tara76 rhodopsin(Pushkarev et al., 2018a). The sequence of Tara76 rhodopsin fragments is the same as ISP44, which was previously reported[31]. We synthesized the target gene through DNA synthesis (Integrated DNA Technologies, Inc., USA) whose codon was optimized for *E. coli*, and introduced *Nde* I and *Not* I restriction sites to use the enzymes (New England BioLabs, USA) to clone the DNA into pKA001 (placUV promoter of pMS 107) expression vector. The protein was expressed in *E. coli* strain UT5600. After transformation of *E. coli* strain UT5600, it was grown in Luria-Bertani (LB) medium containing ampicillin (50 μg/ml) at 35°C. After overnight culture, 1% (5 ml) of the total volume was transferred to 500 ml LB medium containing ampicillin (50 μg/ml) at 35°C, underwent aeration for 200 rpm and was grown to an optical density (OD) of 0.4 at 600 nm. The protein expression was induced by adding 1 mM IPTG (Duchefa Biochemie, The Netherlands) and 7 μM all-trans retinal (Sigma, USA) for 4-6 hours at 35°C. Cells were

harvested for 15 min at 5,000 x g (Eppendorf centrifuge 5810R), washed with buffer (150 mM NaCl, 50 mM Tris-HCl, pH 7.0) and spined down for 20 min at 4,000 x g.

Protein purification

The harvested cells were lysed by sonication and the pellet removed by ultra-centrifugation (Beckman ultracentrifuge). The pellet was suspended in sonication buffer and treated with 2% n-dodecyl-α-D-maltopyranoside (DDM; Anatrace, USA) for solubilization overnight at 4°C. Ultra-centrifugation was performed again for 20 min at 20,000 x g, and Ni^{2+}-NTA agarose (Qiagen) resin was added to the supernatant before incubating with gentle shaking for 4 hours at 4°C. The 6x His-tagged rhodopsins were purified using affinity chromatography. The purified rhodopsin was concentrated using an Amicon Ultra-4 10 K centrifugal filter tube and kept at 4°C.

Absorption spectroscopy at various pH and pKa values

Absorption spectroscopy was used to measure the absorbance of Tara76 rhodopsin using an UV-visible spectrophotometer (UV-2550; Shimadzu, Japan). To titrate the pKa of the primary proton acceptor, the absorption spectra were measured at pH 4 to 10. Based on the data collected, the corrected ratio of protonated and deprotonated forms was obtained at different pH using the calibration curve from the position of the absorption maximum of the mixture. It was calculated with functions containing pKa components ($y=A/(1+10^{pH-pKa})$) using Oigin.9.0.

Proton pump assay

The cells were centrifuged at 5,000 x g for 15 min, washed with an unbuffered solution (10 mM NaCl, 10 mM $MgSO_4$, 10 μM $CaCl_2$) and centrifuged at 4,000 x g for 15 min (Eppendorf centrifuge 5810R). This was repeated three times. The whole cells were diluted to a final concentration of 15 OD/1 ml and 3 ml was used for each measurement. A shortwave cutoff filter (>440 nm, Sigma Koki SCF-50S-44Y, Japan) was used to illuminate the samples. The pH was monitored (Horiba pH meter F-51, Japan) and the data recorded automatically using the Horiba data Navi program (Japan). To compare the amount of movement, measurements were made three times in each sample.

Thermal stability measurements

To measure the thermal stability, we measured the concentration of purified membrane protein. The exact temperature of the water bath was adjusted using an electronic thermometer and a mercury thermometer. After removing the denatured and aggregated protein at 5,000 x g for 30 s, the spectra were measured using an UV-visible spectrophotometer (UV-2550; Shimadzu, Japan) and their values summarized using Oigin.9.0.

pH resistance measurements

To determine the pH resistance, we obtained the maximum absorption spectrum for each purified membrane protein. We changed the pH of each sample with HCl and NaOH, and measured absorption using an UV-visible spectrophotometer (UV-2550; Shimadzu, Japan). High concentrations of HCl or NaOH were used for each pH to prevent dilution. Before measurement, denatured and aggregated proteins were removed by centrifugation.

Detergent resistance measurements

To determine the detergent resistance, each sample was sonicated and cell fragments obtained by ultra-centrifugation (Beckman ultracentrifuge). Protein solubilization was performed with 2% DDM (Anatrace, USA), Triton-X 100 (Sigma-Aldrich) and SDS (Bio-Rad). The solubilization process is time-dependent and was measured with an UV-visible spectrophotometer (UV-2550; Shimadzu, Japan).

Transverse urea gradient gel electrophoresis (TUG-GE)

Gels were prepared vertically using an 8 M gradient gel mixture (29:1 acrylamide solution, electrophoresis buffer, 10% ammonium persulfate [APS], TEMED, 43 mM imidazole/HEPES buffer [pH 7.2-7.8], 0.4% bromophenol blue dye, 8 M urea) from 0 M gradient gel mixture using a Bio-Rad gel caster. The sample was loaded on the gel and run for 15 hours at 20 mA before being visualized using Coomassie R25.

Measurement of electric current

To observe the stability of our proteins against heating effect, we prepared proteins solution (2mg/ml) in distilled water. Then we immersed 1-cm^2 filter paper (100, Hyundai Micro) into the protein solutions for 30 min to allow the proteins to be absorbed into the porous structure of the filter paper. The protein-papers were dried for 4 hours at room temperature along with silica gel. The filter paper we used has a pore size of 3-5 μm and a thickness of approximately 150 μm. After the drying process, each protein-paper was inserted between conductive electrodes (indium tin oxide [ITO] glass; 60 Ω) and a compression force of roughly 100 N was applied to create good contact (Figure 6C inset). The temperature was controlled using a Lakeshore 311 system. The protein samples were heated to the target temperature and incubated for 3 min before measuring the electrical current flow through a sample. The electrical current flow across dried proteins was measured using a source meter (Keithley 2400).

QUANTIFICATION AND STATISTICAL ANALYSIS

Progress under each condition for protein stability experiments

For the measurement of the pH resistance test, the detergent resistance test, and thermal stability for protein stability test, was repeated three times as a comparison target of each protein, such as GR, PR, and TR. The standard deviation values of the data were measured and compared with each other. Each measurement was conducted by converting the amount of reduction for each condition of the maximum absorbance into a ratio. In the dual condition, proteins of the same concentration were prepared and measured under each condition, and three different samples were repeatedly measured to compare the average values, and the standard deviation for this was indicated in the figure. The value of 3 has been experimented with different samples, and this was analyzed through Origin.9.0 software.

Protein stability measurement over time

For the measurement of protein stability for over time, three repeated experiments were performed in each sample and condition, and other conditions were specified identically. It was measured at a constant time, and this was carried out through a comparison of the maximum absorbance of rhodopsin. These analysis values were calculated through the Origin.9.0 software.

Accession numbers

Databases at the National Center for Biotechnical Information (NCBI) at the National Library of Medicine (NCBI) (GR: GenBank accession no. WP_011140202.1, PR: GenBank accession no. Q9F7P4.1, TR: GenBank accession no. WP_014629850.1).